DOI: 10.4081/aiua.2024.13194

ORIGINAL PAPER

Effectiveness of cognitive fusion transrectal ultrasound prostate biopsy when compared with final prostatectomy histology

Ana Sofia Araújo [1], João Serra [2], Sara Anacleto [1], Ricardo Rodrigues [1], Catarina Tinoco [1], Andreia Cardoso [1], Mariana Capinha [1], Vera Marques [1], Paulo Mota [1, 2]

[1] Hospital de Braga, Dept. of Urology, Braga, Portugal;
[2] School of Medicine, University of Minho, Department of Urology, Braga, Portugal.

Summary *Introduction and objectives: Prostate cancer (PCa) is the second most commonly diagnosed cancer in men. Cognitive fusion transrectal ultrasound prostate biopsy is one of several modalities for diagnosing this disease. However, no existing studies have shown the clear superiority of one image-guided technique over another. This investigation aimed to evaluate the efficacy of targeted biopsy through cognitive guidance, as well as to assess the accuracy of multiparametric magnetic resonance imaging (mpMRI) in the detection of PCa compared to the specimen obtained by radical prostatectomy (RP).*

Materials and methods: We conducted a retrospective observational single-center study approved by the ethical committee, including men with prostate-specific antigen (PSA) levels between 2-10 mg/ml who underwent RP and cognitive fusion biopsy (CFB) between 2017 January and 2022 January.

Results: A total of 639 patients were analyzed, 83 of whom met the inclusion criteria and were enrolled in this study. The overall rate of PCa detection with CFB was 79.5% (median of specific PCa detection was 100%), and the rate of detecting clinically significant prostate cancer (csPCa) was 74.7%. In addition, there was 42.2% agreement between the International Society of Urological Pathology (ISUP) score of the CFB and the RP specimen, which increased to 56.6% when the systematic biopsy was added. Regarding the accuracy of mpMRI, several parameters were evaluated with respect to RP sample histology. Of these, tumor location had a total match rate of 39.8% and a partial match rate of 55.4%. Moreover, regarding extraprostatic extension (EPE), the present study found a significant association between the RP specimen and mpMRI ($p = 0.002$), with an agreement rate of 60% if it was present in the histology and 79.5% if it was not. Additionally, larger prostates and tumors located in the transition zone were significantly associated with a lower CFB accuracy ($p = 0.001$ and $p = 0.030$, respectively). After adjusting for all variables evaluated, only prostate volume remains statistically significant ($p = 0.029$).

Conclusions: In this study, we conclude that mpMRI is highly accurate, allowing good characterization of suspicious tumors and reasonably guiding cognitive biopsy. However, the use of both targeted biopsy through cognitive guidance and systematic biopsy increases the diagnostic accuracy for PCa. Although there is no recommendation in the current literature for one guiding technique over another, we believe that cognitive-guided biopsy should only be reserved for centers with no access to ultrasound or magnetic resonance fusion software.

KEY WORDS: *Cognitive fusion biopsy; Diagnostic accuracy; Image fusion prostate cancer; Multiparametric magnetic Resonance imaging; Radical prostatectomy.*

Submitted 2 October 2024; Accepted 6 october 2024

INTRODUCTION

Prostate cancer (PCa) is the second most common solid tumor in males worldwide and tends to be diagnosed mainly after 65 years of age (1). There is considerable variation between developed and developing countries regarding its incidence and mortality due to the hereditary component of the disease, the method of screening and diagnosis, and the involved environmental factors (2, 3). Approximately 95% of tumors are adenocarcinomas and tend to be located in the *peripheral zone* (PZ) of the prostate (4-6). PCa is diagnosed via direct sampling obtained by prostate biopsy, which can be performed transperineally or transrectally, both of which are comparable in terms of tolerability and the detection rate of *clinically significant PCa* (csPCa) (7). However, the first approach is preferred due to the lower risk of infection and associated rectal bleeding and the need for prophylactic antibiotic therapy (8-12). Other complications include urinary retention, haematuria, haematospermia, perineal pain, lower urinary tract symptoms, erectile dysfunction, and, very rarely, death (13).

The decision to perform a prostate biopsy is not only based on a particular *prostate-specific antigen* (PSA), but it is recommended to contextualize with PSA velocity and density, free/total PSA ratio, *digital rectal examination* (DRE), and with some patient risk factors such as age, ethnicity, family history, and associated comorbidities (14, 15).

The classical technique for obtaining a prostate sample is the standard ultrasound-guided double sextant prostate biopsy, where prostatic material (usually 12 samples) is randomly collected at predefined locations (10, 15-17). The limitations associated with this technique include the high rate of *clinically insignificant PCa* (cisPCa) detection

and the failure to detect csPCa which leads to imprecision in stratifying this disease and may require a repeat of the procedure, delaying diagnosis and therapeutic decision-making (10, 12, 15, 16, 18).

Multiparametric magnetic resonance imaging (mpMRI) has shown superiority over individual MRI sequences, allowing the determination of a definitive correlation between the lesions identified by imaging and the tumor location in the specimens obtained from *radical prostatectomy* (RP) (10, 15, 19-21). mpMRI sequences include high-resolution *T2-weighted imaging* (T2W) to describe the anatomy of the prostate, typically combined with two functional MRI techniques, *diffusion-weighted imaging* (DWI) to display cell densities, and *dynamic contrast-enhanced MRI* (DCE-MRI), which can reveal the vascularization at the suspected location (7, 22, 23). The clinical indications for prostatic imaging include detection and localization of PCa, for guidance in *mpMRI-guided biopsy* (mpMRI-GB), local staging and stratification of the tumor, and assessment of PCa recurrence and local treatment (12, 14). It has been demonstrated that the use of mpMRI before biopsy increases the detection of csPCa, and so the *European Association of Urology* (EAU) recommends performing mpMRI before biopsy for all eligible patients (8, 9, 15, 20, 24, 25).

The ability to detect and delineate lesions strongly suggestive of PCa on mpMR images has led to the development of new *magnetic resonance imaging-guided biopsy* (MRI-GB) techniques: *cognitive fusion biopsy* (CFB), biopsy performed during mpMRI imaging, and software fusion biopsy of the images previously obtained mpMRI with the images acquired during the ultrasound (7, 8, 15, 26). CFB consists of lesion identification and delineation on previously obtained mpMRI based on anatomical points that may exist near the lesion (7, 27).

Subsequently, through ultrasound, the operator can direct the biopsy needle to the suspected site, cognitively correlating the images obtained from mpMRI and ultrasound in real time (9, 28). This is an old, fast, simple, and accessible technique that does not require additional software to merge the mpMR images with those of the ultrasound (7, 10, 15, 28). The associated disadvantages are the limited accuracy of the biopsy in the absence of reference points, especially for smaller, anterior-located lesions (7, 9). CFB seems to be more useful for larger and more aggressive lesions, as well as diffuse abnormalities located in the PZ of the prostate (7, 9). The diagnostic accuracy of CFB depends on the visibility of the lesion on the ultrasound images, the position of the patient, and the location of the lesion on mpMRI because ultrasound and mpMRI do not employ the same exploration planes. Furthermore, this technique depends on the operator and his experience in interpreting images and in transposing them to ultrasound (9, 10, 28).

Therefore, taking into account the associated advantages and disadvantages, the present study aims to evaluate the effectiveness of CFB in the detection of PCa in terms of accuracy and diagnosis of csPCa, as well as in comparison with the histological results obtained after RP; it also aims to evaluate the accuracy of mpMRI as well as the parameters that influence the probability of detecting PCa on mpMRI with respect to CFB histology.

Materials and methods

The present study was approved by the *Ethics Committee of Hospital de Braga* (CEHB) (Appendix I) and the *Department of Data Protection* (Appendix II). The norms and recommendations of the Declaration of Helsinki, the Convention on Human Rights and Biomedicine, and the Guidelines on Good Clinical Practice were respected.

We conducted a retrospective observational single-center study, including men who underwent RP and CFB between 2017 January and 2022 January. In addition, the inclusion criteria for this study were: first biopsy, PSA levels between 2 and 10 ng/ml, and lesion categorization on mpMRI according to version 2.1 of the *Prostate Imaging-Rating and Data System* (PI-RADS) equal to or greater than 3. Patients who did not meet the inclusion criteria described above, as well as those whose outcome information was not fully available, were excluded.

Data analysis was performed using IBM®SPSS® software, version 28.0. In the descriptive analyses, *means* (Ms) and *standard deviations* (SDs) are calculated for continuous variables with normal distributions, and *medians* (Mdns) with percentiles (P_{25}-P_{75}) are calculated otherwise. The decision criteria were the skewness coefficient within the interval [-1; 1] and the analysis of the histogram.

Categorical variables are described with numbers (n) and percentages (%). Ordinal variables are described as frequencies and percentages or as medians and percentiles, whichever was more intuitive for describing the variable. When comparing categorical variables, the chi-square test (χ^2) was used in cases of compliance with Cochran's rules; otherwise, Fisher's exact test was used.

The standardized residuals, $Ri = \frac{O_{ij}-E_{ij}}{\sqrt{E_{ij}}}$ (O = observed frequency in the sample, E = expected frequency), were calculated in cases in which the association was statistically significant in tables with dimension (2 + n) X (2 + n), for n > 0. The residuals were said to be statistically significant when ri ≥ |1.96|, under the assumption of a normal distribution. To assess the agreement of the evaluation methods, Cohen's kappa (κ) was calculated, in which 0.01 to 0.20 was considered minimal agreement, 0.21 to 0.40 fair agreement, 0.41 to 0.60 moderate agreement, 0.61 to 0.80 substantial agreement and 0.81 to 1.00 high agreement. Logistic regression was used to evaluate the association of different variables with lower detection of PCa on CFB, first with univariate models and then with models adjusted to the variables with statistically significant results in the univariate analysis. The *odds ratio* (OR) was calculated to assess the association between the variables. Statistical significance was assessed using the 95% *confidence interval* (CI) for the OR and the associated p value. Statistical significance was set at a p value < 0.05.

Definitions

We defined as a csPCa when the *International Society of Urological Pathology* (ISUP) score was greater than or equal to 2. The presence of *extraprostatic extension* (EPE) was identified in the mpMRI report and in the pathological anatomy report of the specimens obtained by RP.

Regarding the characteristics of the lesions on mpMRI and in the histological analysis of the RP sample, 3 parameters were defined with regard to the location of the nodule

with the largest dimensions: zone (peripheral/transition/both), laterality (right, left, both) and site (apex, middle, base, middle+base, middle+apex, base+apex, > 2 sites). If the three location parameters agreed between mpMRI and the RP analysis, we consider a perfect match; if one of the three parameters was not in agreement, mpMRI was said to have no match. A partial match was subdivided into false-positives (all those individuals whose tumor location in the mpMRI report was more extensive than that in the pathological anatomy report for the prostate specimen) and false-negatives (individuals whose imaging indicated a more restricted location than to the actual location of the tumor in the prostate).

Results

Patient selection and sample characterization

The patient selection process is described in the flowchart below (Figure 1).

Of the 639 patients initially analyzed, 83 with a mean age of 64 years were included, 34 of whom (41.0%) were suspected of PCa according to the DRE.

The median total PSA was 6.62 ng/ml (P_{25}-P_{75}, 4.63-8.99), the median free/total PSA ratio was 13.00% (P_{25}-P_{75}, 8.20%-19.00%) and the median PSA density was 0.15 ng/ml/cm^3 (P_{25}-P_{75}, 0.10-0.21).

mpMRI analysis showed that most patients had only 1 suspicious nodule (n = 61, 73.5%), and the mean diameter of the largest identified lesion was 14.27 mm (SD = 4.60).

The median prostatic volume verified on mpMRI was 40.00 cm^3 (P_{25}-P_{75}, 32.00-52.00), and the PI-RADS evaluation classified the largest nodule detected into three categories: 3 (n = 15, 18.1%), 4 (n = 36, 43.4%) and 5 (n = 32, 38.6%).

In most cases, two fragments (n = 58, 69.9%) were collected by CFB, with a range between 0 (n = 17, 20.5%) and 4 (n = 1, 1.2%) samples. Most patients had two positive fragments (n = 36, 43.4%), and the median number of positive samples was 2.00 (P_{25}-P_{75}, 1.00-2.00).

Regarding SB, the most common number of fragments collected was 12 (n = 76, 91.6%). The tumor was detected in 0-2 (n = 15, 18.1%), 3-5 (n = 31, 37.3%), 6-7 (n = 19, 22.9%) and ≥ 8 samples (n = 18, 21.7%), with a median of 5.00 samples (P_{25}-P_{75}, 3.00-7.00).

On mpMRI, the nodules were mostly found in the PZ (n = 63, 75.9%), on the left (n = 37, 44.6%), and in the apical region (n = 23, 27.7%). In the RP sample, the tumor was detected more frequently in the PZ (n = 64, 77.1%), bilaterally (n = 45, 54.2%), and in more than 2 sites (n = 22, 26.5%).

The PCa ISUP score obtained for the samples collected from SB was distributed among categories 1 (n = 12, 14.5%) to 5 (n = 11, 13.3%), with most classified as category 4 (n = 17; 20.5%).The same results were observed for the tumors detected with CFB, with ISUP scores from 1 (n = 20, 24.1%) to 5 (n = 6, 7.2%), with category 4 being more frequent (n = 22, 26.5%). The overall ISUP scores were distributed among the same categories, from 1 (n = 15, 18.1%) to 5 (n = 13, 15.7%), where the highest frequency was observed for ISUP category 2 (n = 24, 28.9%).

For the samples obtained from RP, the ISUP carcinoma scores ranged from 1 (n = 4, 4.8%) to 5 (n = 19, 22.9%), with most classified into category 2 (n = 29, 34.9%).

Regarding the presence of EPE, we found that 29 (34.9%) and 25 (30.1%) patients were positive on mpMRI and post-RP, respectively.

Following SB, 16 individuals (19.3%) were negative for tumor detection in the collected fragments, 12 (14.5%) were classified as having cisPCa, and 55 individuals (66.3%) had csPCa.

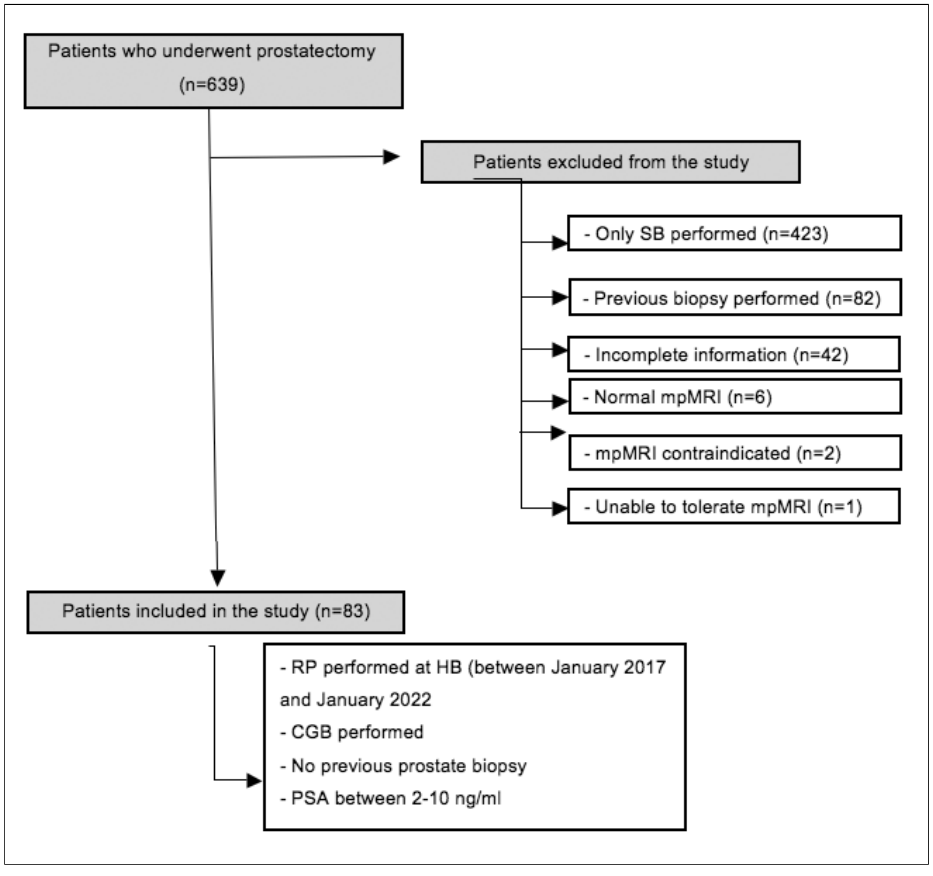

Figure 1.
Flowchart of the patient selection according to the inclusion and exclusion criteria for the study.

Regarding the samples obtained by CFB, 20 (24.1%) and 62 men (74.7%) were said to have cisPCa and csPCa, respectively; only 1 patient (1.2%) had no diagnosis of PCa. After removal of the prostate via RP, 4 men (4.8%) were diagnosed with cisPCa, and 79 individuals (95.2%) had csPCa (Table 1).

Table 1.
Sample characterization.

Parameters	N = 83
Age	64.40 (6.08) [49-77]
Digital rectal examination	
Normal	49 (59.0%)
Suspected	34 (41.0%)
Total PSA (ng/ml)	6.62 (4.63–8.99) [2.10–10.00]
Free/total PSA Ratio (%)	13.00 (8.20–19.00) [4.37–82.90]
PSA density (ng/ml/cm^3)	0.15 (0.10–0.21) [0.05–0.42]
Number of nodules on mpMRI	
1	61 (73.5%)
2	16 (19.3%)
≥ 3	6 (7.2%)
Diameter of the largest nodule on mpMRI (mm)	14.27 (4.60) [11.00–17.00]
Prostate volume (cm^3)	40.00 (32.00–52.00) [18.00–97.00]
PI-RADS category	
3	15 (18.1%)
4	36 (43.4%)
5	32 (38.6%)
Number of samples collected by CFB	
1	3 (3.6%)
2	58 (69.9%)
3	14 (16.9%)
4	7 (8.4%)
5	1 (1.2%)
Number of tumor-bearing samples collected by CFB	2.00 (1.00–2.00) [0.00–4.00]
0	17 (20.5%)
1	18 (21.7%)
2	36 (43.4%)
3	11 (13.3%)
4	1 (1.2%)
Number of fragments collected by SB	
10	5 (6.0%)
11	2 (2.4%)
12	76 (91.6%)
Number of tumor-bearing fragments collected by SB	5.00 (3.00–7.00) [0-12]
0–2	15 (18.1%)
3–5	31 (37.3%)
6–7	19 (22.9%)
≥ 8	18 (21.7%)
Location of the nodule on mpMRI Zone	
PZ	63 (75.9%)
TZ	14 (16.9%)
Both (PZ + TZ)	6 (7.2%)
Laterality	
Right	28 (33.7%)
Left	37 (44.6%)
Bilateral	18 (21.7%)
Site	
Apex	23 (27.7%)
Middle	19 (22.9%)
Base	14 (16.9%)
Middle + Apex	11 (13.3%)
Middle + Base	5 (6.0%)
Base + Apex	2 (2.4%)
> 2 sites	9 (10.8%)
Location of the nodule in the RP sample Zone	
PZ	64 (77.1%)
TZ	12 (14.5%)
Both (PZ + TZ)	7 (8.4%)
Laterality	
Right	19 (22.9%)
Left	19 (22.9%)
Bilateral	45 (54.2%)
Site	
Apex	17 (20.5%)
Middle	14 (16.9%)
Base	13 (15.7%)
Middle + Apex	11 (13.3%)
Middle + Base	4 (4.8%)
Base + Apex	2 (2.4%)
> 2 sites	22 (26.5%)
ISUP score from SB	
1	12 (14.5%)
2	14 (16.9%)
3	13 (15.7%)
4	17 (20.5%)
5	11 (13.3%)
ISUP score from CSB	
1	20 (24.1%)
2	18 (21.7%)
3	16 (19.3%)
4	22 (26.5%)
5	6 (7.2%)
Global ISUP score	
1	15 (18.1%)
2	24 (28.9%)
3	19 (22.9%)
4	12 (14.5%)
5	13 (15.7%)
ISUP score from RP	
1	4 (4.8%)
2	29 (34.9%)
3	27 (32.5%)
4	4 (4.8%)
5	19 (22.9%)
EPE on mpMRI	
Yes	29 (34.9%)
No	54 (65.1%)
EPE on RP samples	
Yes	25 (30.1%)
No	58 (69.9%)
SB PCa	
None	16 (19.3%)
cisPCa	12 (14.5%)
csPCa	55 (66.3%)
CFB PCa	
None	1 (1.2%)
cisPCa	20 (24.1%)
PcsPCa	62 (74.7%)
RP PCa	
cisPCa	4 (4.8%)
csPCa	79 (95.2%)

For continuous variables, the results are presented as M (SD) [min-max] for normal distributions and Mdn (P_{25}–P_{75}) [min-max] for nonnormal distributions; categorical variables are presented as n (%).

Overall and specific rate of PCa detection

Table 2 presents the results of the overall and specific rate of PCa detection for CFB. The overall rate of CaP detection

Table 2.
Overall and specific rate of PCa detection.

PCa Detection	
Overall	66 (79.5%)
Specific	
1 - No. fragments collected – No. positive fragments / No. fragments collected	100% (50.0% - 100%) [0.0% - 100%]
0.0%	17 (20.5%)
33.0%	2 (2.4%)
40.0%	1 (1.2%)
50.0%	13 (15.7%)
75.0%	2 (2.4%)
100%	48 (57.8%)

Continuous variables are presented as M (SD) [min-max] for normal distributions and Mdn (P_{25}-P_{75}) [min-max] for nonnormal distributions; categorical variables are presented as n (%).

(obtained by the presence of ≥ 1 positive sample(s) in the total number of samples collected) was 79.5%. The median of the specific rate of PCa detection, calculated by the formula $(1 - \frac{\text{No. fragments collected} - \text{No. positive fragments}}{\text{No. fragments collected}})$, was 100% ($P_{25}$-$P_{75}$, 50.0%-100.0%). For instance, if it was collected 3 fragments and all of them were positive $[1 - (\frac{3-3}{3})] = (1-0) = 1$ or 100%. Otherwise, if it was collected 3 fragments but none of them were positive $[1 - (\frac{3-0}{3})] = (1-1) = 0$ or 0.0%.

Association of PCa detection between CFB and SB

The association of cancer detection between CFB and SB showed moderate agreement ($\kappa = 0.36$), with statistical significance ($p < 0.001$), mainly for csPCa (80.6%) (Table 3). The standardized residues suggested that the number of samples considered to not have tumor tissue according to CFB and to have cisPCa according to SB was higher than expected (n = 1, 100%, Ri = 2.2%).
The proportion of cisPCa detected by both CFB and SB was 40.0%, with a positive residue of Ri = 3.0, suggesting a higher proportion than expected. In contrast, the proportion of cisPCa from CFB classified as csPCa by SB (25.0%) was lower than expected (ri = -2.3). Although significant, 4.8% of csPCas detected with CFB were considered csPCa according to SB, which was lower than expected (ri = -2.0).

Comparison of the ISUP scores obtained with CFB and the Global ISUP score with the ISUP score obtained with RP histology

Table 4 compares the ISUP scores obtained for the samples collected with CFB with those described in the RP histology, using the formula (ISUP RP-ISUP CFB), with total agreement observed for 35 (42.2%). The proportions of -/+1 and -/+2 errors were 45.7% (38 individuals) and 12% (10 individuals), respectively. The same analysis was performed for the Global ISUP score, yielding a total agreement for 47 patients (56.6%), and proportions of -/+1, -/+2 and -/+3 errors of 30.1% (25 patients), 10.8% (9 patients) and 2.4% (2 patients), respectively.

Table 4.
Comparison of the ISUP scores obtained with CFB and the Global ISUP score with the ISUP score obtained with RP histology.

	ISUP RP–ISUP CFB		ISUP RP–ISUP Global	
	n	%	n	%
-3	0	0.0%	1	1.2%
-2	2	2.4%	3	3.6%
-1	9	10.8%	5	6.0%
0	35	42.2%	47	56.6%
1	29	34.9%	20	24.1%
2	8	9.6%	6	7.2%
3	0	0.0%	1	1.2%

Rate of match considering mpMRI locations relative to RP histology

With respect to the RP samples, mpMRI had total match in tumor location in 33 patients (39.8%). Partial match was achieved for 46 patients (55.4%), 40 (48.2%) with false negatives and 6 (7.2%) with false positives. No match at all was obtained for 4 patients (4.8%) (Figure 2).

Figure 2.
Rate of match considering mpMRI locations relative to RP histology.

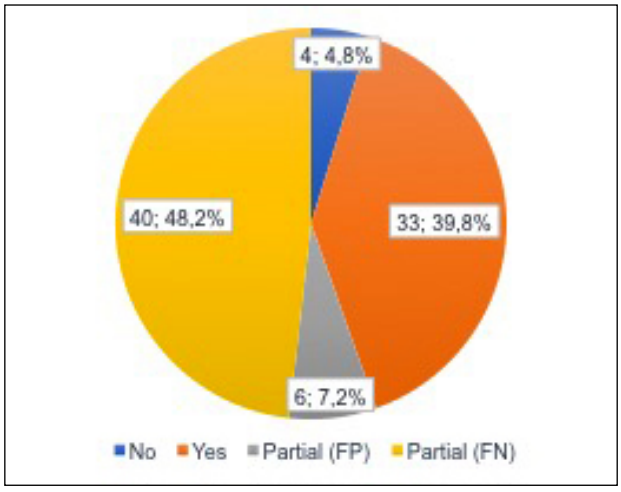

Table 3.
Association of PCa detection between CFB and SB.

	PCa detected by CFB				
PCa detected by SB	None	cisPCa	csPCa	Fisher's exact test	Cohen's κ
None	0 (0.0%)	7 (35.0%)	9 (14.5%)	p < 0.001	0.36
cisPCa	1 (100%), Ri = 2.2	8 (40.0%), Ri = 3.0	3 (4.8%), Ri = -2.0		
csPCa	0 (0.0%)	5 (25.0%), Ri =- 2.3	50 (80.6%)		

Association of laterality, tumor zone, site and EPE observed in RP histology with that observed on mpMRI

The laterality in the RP histology was statistically significantly associated with the laterality on mpMR ($p < .001$).
The agreement for right-, left-, and bilaterally located tumors was 73.7%, 94.7% and 28.9%,

Table 5.
Association of laterality observed in RP histology with that observed on mpMRI.

	RP histology laterality				
	Right	Left	Both	Fisher's exact test	Cohen's κ
Zone according to mpMRI					
Right	14 (73.7%)	0 (0.0%)	14 (31.1%)	p < 0.001	0.35
Left	1 (5.3%)	18 (94.7%)	18 (40.0%)		
Both	4 (21.1%)	1 (5.3%)	13 (28.9%)		

Table 6.
Association of tumor zone in RP histology with that identified on mpMRI.

	Zone according to RP histology				
	PZ	TZ	Both	Fisher's exact test	Cohen's κ
Zone according to mpMRI					
PZ	61 (95.3%)	0 (0%)	2 (28.6%)	p < 0.001	0.84
TZ	2 (3.1%)	12 (100%)	0 (0%)		
Both	1 (1.6%)	0 (0%)	5 (71.4%)		

respectively. Cohen's κ was 0.35, indicating slight agreement (Table 5).
The zone in which the tumor was found in RP histology was statistically significantly associated with that identified on mpMRI (p < 0.001). The agreement for the PZ, TZ, and both was 95.3%, 100% and 71.4%, respectively. Cohen's κ was 0.84, indicating high agreement (Table 6).
Table 7 shows the associations of the RP histological site with that identified on mpMRI. Statistically significant differences were found for apical (p = 0.026), middle (p < 0.001), and basal locations (p < 0.001) and > 2 sites (p < 0.001). Cohen's k showed the highest agreement for the basal location (κ = 0.80, high), with true negatives of 93.8% and true positives of 89.5%. This was followed by agreement in middle locations (κ = 0.70, substantial), which had the highest proportion of true positives (89.7%), and in > 2 sites (κ = 0.43, fair), which had the highest proportion of true negatives (98.4%). Finally, apical sites had an agreement of 0.20, with 62.0% true negatives and 75.0% true positives.
The association of EPE assessed by RP histology with that assessed on mpMRI was statistically significant (p = 0.002) (Table 8). Regarding positive EPE as observed in RP histology, 60.0% of cases were also positive on mpMRI. When EPE was not detected in the RP specimen, it was also not detected in 75.9% of the cases on imaging.
The agreement between the two modalities was fair (κ = 0.34).

Table 7.
Association of tumor zone in RP histology with that identified on mpMRI.

	Apex RP histology		Statistical test	
Apex mpMRI	No	Yes	X^2 test	Cohen's κ
No	44 (62.0%)	3 (25.0%)	p = 0.026	0.20
Yes	27 (38.0%)	9 (75.0%)		
	Middle RP histology			
Middle mpMRI	No	Yes	X^2 test	
No	45 (83.3%)	3 (10.3%)	p < 0.001	0.70
Yes	9 (16.7%)	26 (89.7%)		
	Base RP histology			
Base mpMRI	No	Yes	X^2 test	
No	60 (93.8%)	2 (10.5%)	p < 0.001	0.80
Yes	4 (6.3%)	17 (89.5%)		
	> 2 sites RP histology			
> 2 sites mpMRI	No	Yes	X^2 test	
No	60 (98.4%)	14 (63.6%)	p < 0.001	0.43
Yes	1 (1.6%)	8 (36.4%)		

Table 8.
Association of EPE assessed by RP histology and that assessed on mpMRI.

	EPE RP histology			
	No	Yes	X^2 test	Cohen's κ
EPE mpMRI				
No	44 (75.9%)	10 (40.0%)	p = 0.002	0.34
Yes	14 (24.1%)	15 (60.0%)		

Association of different variables with lower detection of PCa on CFB, adjusted for covariates

Table 9 shows the association of different variables with no detection of PCa on CFB, adjusted for covariates.
In the univariate analysis, covariates referring to the presence of csPCa in the RP specimen (OR = 0.07 [95% CI = 0.07; 0.74], p = 0.027), a suspected tumor from DRE (OR

Table 9.
Association of different variables with lower detection of PCa on CFB, adjusted for covariates.

	Dependent variable: No detection of PCa on CBF	
	Unadjusted models (univariate)	Ajusted model
Age	OR = 1.04 (p = 0.440) [95% CI = (0.95; 1.14)]	-
Suspected tumor on DRE	OR = 0.14 (p = 0.014) [95% CI = (0.03; 0.67)]	OR = 0.30 (p = 0.166) [95% CI = (0.06; 1.64)]
Total PSA	OR = 0.99 (p = 0.925) [95% CI = (0.79; 1.24)]	-
Free/total PSA Ratio	OR = 1.02 (p = 0.477) [95% CI = (0.97; 1.06)]	-
PSA density	OR = 0.001 (p = 0.033) [95% CI = (0.00; 0.51)]	-
Number of nodules	OR = 1.39 (p = 0.393) [95% CI = (0.66; 2.94)]	-
Size of the largest nodule	OR = 0.96 (p = 0.459) [95% CI = (0.85; 1.08)]	-
Prostate volume	OR = 1.06 (p = 0.001) [95% CI = (1.02; 1.09)]	OR = 1.04 (p = 0.029) [95% CI = (1.00; 1.08)]
PI-RADS category	OR = 0.46 (p = 0.045) [95% CI = (0.22; 098)]	OR = 0.92 (p = 0.848) [95% CI = (0.37; 2.27)]
Site: Apex	OR = 0.47 (p = 0.199) [95% CI = (0.15; 1.49)]	-
Site: Middle	OR = 0.95 (p = 0.926) [95% CI = (0.32; 2.80)]	-
Site: Base	OR = 1.86 (p = 0.292) [95% CI = (0.59; 5.85)]	-
> 2 sites	OR = 2.14 (p = 0.320) [95% CI = (0.48; 9.63)]	-
Zone: PZ	OR = 0.25 (p = 0.017) [95% CI = (0.08-0.78)]	OR = 0.46 (p = 0.524) [95% CI = (0.03; 4.98)]
Zone: TZ	OR = 3.96 (p = 0.030) [95% CI = (1.15; 13,66)]	OR = 1.11 (p = 0.936) [95% CI = (0.09; 14.61)]
Both (PZ + TZ)	OR = 2.07 (p = 0.426) [(95% CI = 0.35; 12,36)]	-
csPCa on RP	OR = 0.07 (p = 0.027) [95% CI = (0.07; 0.74)]	OR = 0.12 (p = 0.111) [95% CI = (0.009; 1.63)]

= 0.14 [95% CI = 0.03; 0.67], p = 0.014) and PSA density (OR = 0.001 [95% CI = (0.00; 0.51)], p = 0.033) were significantly associated with detection of PCa on CFB. A higher PI-RADS classification (OR = 0.46 [95% CI = 0.22; 098], p = 0.045) and tumor location in the PZ (OR = 0.25 [95% CI = (0.08-0.78)], p = 0.017) were also associated with detection of PCa on CFB.

However, the volume of the prostate (OR = 1.06 [95% CI = 1.02; 1.09], p = 0.001) and nodule location in the TZ (OR = 3.96 [95% CI = 1.15; 13.66)], p = 0.030) were associated with no detection of PCa on CFB.

When adjusting for all statistically significant variables from the univariate analysis, only prostate volume remained significant in the multivariate analysis (OR = 1.04 [95% CI = 1.01; 1.08)], p = 0.029); that is, for every 1 cm^3 increase in the volume of the prostate, the odds of the CFB not hitting the mpMRI site increased by 4%. The variable related to PSA density was not taken into account in the multivariate model, despite having a statistically significant result in the unadjusted model, as there was a loss of statistical power due to a wide confidence interval without statistical significance.

Discussion

The main objective of this study was to evaluate the effectiveness of CFB in the detection of PCa. We observed an overall rate of PCa detection of 79.5%, consistent with previous investigations. The median specific PCa detection rate in our investigation was 100%, i.e., in 57.8% of the patients, all the biopsied samples were positive for the tumor. A possible explanation for this high value may be the selection of patients with imaging results suggestive of PCa (PI-RADS ≥ 3) and elevated PSA values. *Dekalo et al.* showed that CFB had a PCa detection rate of 52% and 78% in individuals suspected only due to imaging and in men with changes in both analytical and mpMRI results, respectively (29). In the study published by *Wang et al.*, there was a 67% detection rate of PCa through CFB (30). A Portuguese study published in the Ata Urologica Portuguesa revealed an effectiveness of CFB of 73% in the detection of PCa (15). Recently, *Kulis et al.* revealed a 52% success rate of CFB in patients with high PSA levels and persistent changes on imaging despite a previous negative SB (31).

Additionally, it was performed SB and CFB in the same patients which allow the association of these two routes of sample collection regarding the ability to identify prostatic lesions, and statistically significant differences were found with a moderate association between the two. The two methods agreed in the detection of csPCa and cisPCa in 80.6% and 40.0% of cases, respectively.

Based on the analysis of these data, CFB detected 62 cases (74.7%) of csPCa, while SB only detected 55 cases (66.3%). Nevertheless, we found that 9 and 3 patients classified as having no tumor and cisPCa, respectively, according to SB were identified as having csPCa with CFB, i.e., approximately 19.3% of the patients with csPCa in our sample who underwent SB only would not have been correctly identified. According to the available literature, the false-negative rate of SB is between 15.7-17%, especially for csPCa, corroborating the conclusions of several studies that performing a prebiopsy mpMRI allows the detection of more cases of csPCa than with only SB (15, 18, 30-35). However, the 5 patients diagnosed with csPCa by SB but cisPCa according to CFB was greater than expected. These results are in agreement with previous studies, where *Kulis et al.* revealed that if only 5 patients (13.16%) had undergone CFB, the diagnosis would have failed; one of these patients had a Gleason scale score of 8 in the anatomopathological evaluation after RP (31). Thus, the data of the present study suggest that CFB could not detect all cases of csPCa, which is in agreement with previous studies; therefore, we do not advise completely replacing SB with CFB, but instead, they should be used in complementarity to reduce errors in the diagnosis of csPCa (10, 18, 30, 31, 35-38).

Based on the histology of the samples collected with CFB, the greatest Gleason score in the specimen was classified according to the ISUP score; a similar analysis was conducted for tumor tissue present in the prostate specimen collected by RP. When comparing the differences between the ISUP values from RP and CFB for each patient, a total agreement of 42.2% (35 patients) was obtained. *Baco et al.* showed that the agreement in the Gleason score between SB and RP samples was 90% (20). This finding contrasts with the retrospective study by *Diamand et al.*, which showed an agreement of 51.2%; however, the combination of SB and CFB increased the agreement with the final RP histology to 63.2% (39). This conclusion was observed in our study, showing that the combination of CFB and SB increased the agreement to 56.6%, a finding that is also corroborated by multicenter studies that confirmed the benefit of concomitant SB (39, 40).

Another objective of this study was to evaluate the accuracy of data provided from mpMRI in terms of tumor location with respect to the histology of the specimen obtained with RP. A total match between the two was obtained in 39.8% (33 cases), a partial match was achieved in 55.4% (46 cases) and no match at all was found in 4.8% (4 cases). To date, no studies have been conducted comparing the 3 location parameters between mpMRI and RP specimens. When analyzing each of the specific location parameters, we found high agreement with respect to laterality (73.7% on the right and 94.7% on the left) and zone (95.3% in the PZ and 100% in the TZ). With regard to site, Cohen's κ value showed a stronger agreement when the tumor was at the base (positive predictive value (PPV), 89.5%; negative predictive value (NPV), 93.8%), followed by the middle area (PPV 89.7%; NPV 83.3%). Therefore, there are high values in all parameters of the location; however, the total nonagreement can be explained because radiologists and pathologists do not use the same templates to correlate the locations, in addition to the fact that the in vivo and in vitro anatomical positions of the prostate also influence the interpretation of the affected site.

Another way to assess the accuracy of mpMRI is through EPE, comparing it with that reported by the histology of the RP samples. In the present study, agreements of 75.9% and 60% were obtained in detecting the absence and presence of EPE, respectively. These data allow us to infer that in the present study, mpMRI had a specificity of 53% and a sensitivity of 18%. In the study by *Martins et al.*, a sensi-

tivity of 56% (CI, 39%-72%) and a specificity of 84% (CI, 75%-91%) were found. Similar values were found in articles that evaluated the accuracy of mpMRI regarding EPE (41-44). Possible explanations for this wide variation in the accuracy of mpMRI in detecting mpMRI include the fact that there are several classification systems with different criteria for predicting the risk of EPE; however, in validation cohorts, none showed definitive superiority over others (12, 44), and therefore, different criteria can lead to different results. Additionally, differences in the study design and in EPE prevalences among the populations, as well as differences in the experience of the radiologists and the center where the findings are interpreted, may influence the results (43).

We also intended to evaluate which factors (demographic, analytical, physical examination, mpMRI, and histological data of RP) were associated with a lower PCa detection on CFB.

In the present study, age was not found to be a statistically significant predictor of PCa detection on CFB. This can be explained by the findings of *Bura et al.*, who showed that younger men exhibit lower signal intensity on T2W imaging, lower values on DWI, and diffuse enhancement on DCE-MRI, making the interpretation of PCa on mpMRI more difficult. Although we are not aware of the existence of studies that associated DRE findings and the effectiveness of CFB, it is understood that there is a positive association between these two variables; therefore, when the DRE suggests a mass, CFB is more likely to hit the target tumor site.

We also concluded that the PSA value did not affect the PCa detection of the CFB, a result that is corroborated by the study by Guang Xu (45). Possible explanations for this finding are due to the fact that larger prostates are also associated with a higher PSA level and as shown below, prostate volume is associated with a lower PCa detection on CFB. However, PSA density was found to be a significant independent predictor of the correctness of CFB in the detection of PCa in the multivariate regression analysis, as *Pang et al.* and *Dekalo et al.* presented in their studies (10, 29).

Regarding factors related to mpMRI, in previous studies, it was demonstrated that for larger suspected nodules and higher values on the PI-RADS scale, the lesions were more frequently detected with CFB (10, 21, 36, 38, 45). However, in our study, only higher values on the PI-RADS scale were associated with higher PCa detection on CFB. In addition, there was no preferential nodule location of the prostate with statistically significant in the univariate logistic regression model; however, it was demonstrated that malignant lesions in the anterior apical region of the prostate can be more frequently missed (46).

With regard to prostate volume and the presence of cancer in the TZ, they were statistically significantly associated with less PCa detection on CFB. These facts are corroborated by the current literature, since for larger prostates, there is greater difficulty in performing the biopsy (36). The association of TZ lesions with an inaccurate CFB may be due to the difficulty in distinguishing PCa from benign hyperplasia nodules (47). In contrast to TZ lesions, lesions located in the PZ were an independent predictor of PCa detection with CFB (36).

We also concluded that the existence of csPCa in the histology of RP samples was associated with a higher probability of correct PCa detection on CFB, which can be explained by the fact that higher Gleason scores are associated with greater tumor aggressiveness, allowing greater visibility on mpMRI (21, 47, 48) and, therefore, a higher probability of CFB PCa detection.

This study demonstrated several limitations, including those related to its retrospective and nonrandomized nature, such as the potential bias in patient selection. In addition, the small sample size could have implications regarding the inference of the statistical results. Furthermore, factors associated with the performance of the biopsy, the lack of unified criteria in imaging and histology reports, and inconsistent experience by all professionals involved could have influenced these results.

Conclusion

The present study concludes that mpMRI is highly accurate in characterizing the presence of suspicious nodules and reasonably in guiding cognitive biopsy. However, the use of both targeted biopsy through cognitive guidance and systematic biopsy increases the diagnostic accuracy for PCa. Although there is no recommendation in the current literature for one guiding technique over another, we believe that CFB should only be reserved for centers with no access to ultrasound or magnetic resonance fusion software. Finally, more prospective, and randomized studies are needed to validate the results obtained.

References

1. Bray F, Ferlay J, Soerjomataram I, et al. Global cancer statistics 2018: GLOBOCAN estimates of incidence and mortality worldwide for 36 cancers in 185 countries. CA Cancer J Clin. 2018; 68:394-424.

2. Rawla, P. Epidemiology of Prostate Cancer. World J Oncol. 2019; 10:63-89.

3. Haas G, Delongchamps N, Brawley O, et al. The worldwide epidemiology of prostate cancer: perspectives from autopsy studies. Can J Urol. 2008; 15:3866-71.

4. McNeal J, Redwine E, Freiha F, Stamey T. Zonal distribution of prostatic adenocarcinoma. Correlation with histologic pattern and direction of spread. Am J Surg Pathol. 1988; 12:897-906.

5. Grignon J, Sakr W. Zonal origin of prostatic adenocarcinoma: are there biologic differences between transition zone and peripheral zone adenocarcinomas of the prostate gland? J Cell Biochem Suppl. 1994; 19:267-9.

6. Mazhar D, Waxman J. Prostate cancer. Postgrad Med J. 2002; 78:590-5.

7. Puech P, Ouzzane A, Gaillard V, et al. Multiparametric MRI-targeted TRUS prostate biopsies using visual registration. Biomed Res Int. 2014; 2014:819360.

8. Immerzeel J, Israel B, Bomers J, et al. Multiparametric Magnetic Resonance Imaging for the Detection of Clinically Significant Prostate Cancer: What Urologists Need to Know. Part 4: Transperineal Magnetic Resonance-Ultrasound Fusion Guided Biopsy Using Local Anesthesia. Eur Urol. 2022; 81:110-117.

9. Venderink W, Bomers J, Overduin C, et al. Multiparametric Magnetic Resonance Imaging for the Detection of Clinically Significant

Prostate Cancer: What Urologists Need to Know. Part 3: Targeted Biopsy. Eur Urol. 2020; 77:481-490.

10. Pang C, Wang M, Hou H, et al. Cognitive magnetic resonance imaging-ultrasound fusion transperineal targeted biopsy combined with randomized biopsy in detection of prostate cancer. World J Clin Cases. 2021; 9:11183-11192.

11. Sugano D, Kaneko M, Yip W, et al. Comparative Effectiveness of Techniques in Targeted Prostate Biopsy. Cancers (Basel). 2021; 13:1449.

12. EAU Guidelines. Edn. presented at the EAU Annual Congress Amsterdam 2022. ISBN 978-94-92671-16-5.

13. Loeb S, Vellekoop A, Ahmed H, et al. Systematic review of complications of prostate biopsy. Eur Urol. 2013; 64:876-92.

14. Streicher J, Meyerson B, Karivedu V, Sidana A. A review of optimal prostate biopsy: indications and techniques. Ther Adv Urol. 2019; 11:1756287219870074.

15. Pina J, Dias J, Meirinha A, et al. Biópsia prostática dirigida por fusão cognitiva após ressonância magnética multiparamétrica. Comparação com a técnica habitual de biópsia aleatória. Acta Urológica Portuguesa. 2015; 32:101-107.

16. Rodrigues S, Dores M, Metrogos V, et al. Biópsia prostática orientada por fusão de imagem RMN-ETR: breve revisão a propósito de caso clínico. Acta Urológica Portuguesa. 2014; 31:88-91.

17. Hsieh P, Chang T, Lin W, et al. A comparative study of transperineal software-assisted magnetic resonance/ultrasound fusion biopsy and transrectal cognitive fusion biopsy of the prostate. BMC Urol. 2022; 22:72.

18. Ahmed H, Bosaily A, Brown L, et al. PROMIS study group. Diagnostic accuracy of multi-parametric MRI and TRUS biopsy in prostate cancer (PROMIS): a paired validating confirmatory study. Lancet. 2017; 389:815-822.

19. McHugh J, Saunders E, Dadaev T, et al. Prostate cancer risk in men of differing genetic ancestry and approaches to disease screening and management in these groups. Br J Cancer. 2022; 126:1366-1373.

20. Baco E, Ukimura O, Rud E, et al. Magnetic resonance imaging-transectal ultrasound image-fusion biopsies accurately characterize the index tumor: correlation with step-sectioned radical prostatectomy specimens in 135 patients. Eur Urol. 2015; 67:787-94.

21. Turkbey B, Mani H, Shah V, et al. Multiparametric 3T prostate magnetic resonance imaging to detect cancer: histopathological correlation using prostatectomy specimens processed in customized magnetic resonance imaging based molds. J Urol. 2011; 186:1818-24.

22. Israël B, Leest MV, Sedelaar M, et al. Multiparametric Magnetic Resonance Imaging for the Detection of Clinically Significant Prostate Cancer: What Urologists Need to Know. Part 2: Interpretation. Eur Urol. 2020; 77:469-480.

23. Engels RRM, Israël B, Padhani AR, Barentsz JO. Multiparametric Magnetic Resonance Imaging for the Detection of Clinically Significant Prostate Cancer: What Urologists Need to Know. Part 1: Acquisition. Eur Urol. 2020; 77:457-468.

24. Ploussard G, de la Taille A. Prostate biopsies: let's move forward. Eur Urol. 2013; 64:893-4.

25. Wegelin O, Exterkate L, van der Leest M, et al. The FUTURE Trial: A Multicenter Randomised Controlled Trial on Target Biopsy Techniques Based on Magnetic Resonance Imaging in the Diagnosis of Prostate Cancer in Patients with Prior Negative Biopsies. Eur Urol. 2019; 75:582-590.

26. Moore CM, Robertson NL, Arsanious N, et al. Image-guided prostate biopsy using magnetic resonance imaging-derived targets: a systematic review. Eur Urol. 2013; 63:125-40.

27. Siddiqui MM, Rais-Bahrami S, Truong H, et al. Magnetic resonance imaging/ultrasound-fusion biopsy significantly upgrades prostate cancer versus systematic 12-core transrectal ultrasound biopsy. Eur Urol. 2013; 64:713-719.

28. Bjurlin MA, Meng X, Le Nobin J, et al. Optimization of prostate biopsy: the role of magnetic resonance imaging targeted biopsy in detection, localization and risk assessment. J Urol. 2014; 192:648-58.

29. Dekalo S, Matzkin H, Mabjeesh NJ. High cancer detection rate using cognitive fusion - targeted transperineal prostate biopsies. Int Braz J Urol. 2017; 43:600-606.

30. Wang L, Wang X, Zhao W, et al. Surface-projection-based transperineal cognitive fusion targeted biopsy of the prostate: an original technique with a good cancer detection rate. BMC Urology. 2019; 19:107.

31. Kuliš T, Zekulic T, Alduk AM, et al. Targeted prostate biopsy using a cognitive fusion of multiparametric magnetic resonance imaging and transrectal ultrasound in patients with previously negative systematic biopsies and non-suspicious digital rectal exam. Croat Med J. 2020; 61:49-54.

32. Yamada Y, Ukimura O, Kaneko M, et al. Moving away from systematic biopsies: image-guided prostate biopsy (in-bore biopsy, cognitive fusion biopsy, MRUS fusion biopsy) -literature review. World J Urol. 2021; 39:677-686.

33. Ryan J, Broe MP, Moran D, et al. Prostate cancer detection with magnetic resonance imaging (MRI)/ cognitive fusion biopsy: Comparing standard and targeted prostate biopsy with final prostatectomy histology. Can Urol Assoc J. 2021; 15:E483-e487.

34. Watts KL, Frechette L, Muller B, et al. Systematic review and meta-analysis comparing cognitive vs. image-guided fusion prostate biopsy for the detection of prostate cancer. Urologic Oncology: Seminars and Original Investigations. 2020; 38:734.e19-734.e25.

35. Lim LY, Tan GH, Zainuddin ZM, et al. Prospective evaluation of using multiparametric magnetic resonance imaging in cognitive fusion prostate biopsy compared to the standard systematic 12-core biopsy in the detection of prostate cancer. Urol Ann. 2020; 12:276-282.

36. Majchrzak N, Cieslinski P, Milecki T, et al. Analysis of the usefulness of magnetic resonance imaging and clinical parameters in the detection of prostate cancer in the first systematic biopsy combined with targeted cognitive biopsy. Cent European J Urol. 2021; 74:321-326.

37. Oberlin DT, Casalino DD, Miller FH, et al. Diagnostic Value of Guided Biopsies: Fusion and Cognitive-registration Magnetic Resonance Imaging Versus Conventional Ultrasound Biopsy of the Prostate. Urology. 2016; 92:75-9.

38. Pepe P, Pepe L, Panella P, Pennisi M. Can multiparametric ultrasound improve cognitive MRI/TRUS fusion prostate biopsy. Arch Ital Urol Androl. 2020; 92.89-92

39. Diamand R, Oderda M, Al Hajj Obeid W, et al. A multicentric study on accurate grading of prostate cancer with systematic and MRI/US fusion targeted biopsies: comparison with final histopathology after radical prostatectomy. World J Urol. 2019; 37:2109-2117.

40. Ploussard G, Borgmann H, Briganti A, et al.; EAU-YAU Prostate Cancer Working Group. Positive pre-biopsy MRI: are systematic biopsies still useful in addition to targeted biopsies? World J Urol. 2019; 37:243-251.

41. Martins M, Regusci S, Rohner S, et al. The diagnostic accuracy of

multiparametric MRI for detection and localization of prostate cancer depends on the affected region. BJUI Compass. 2021; 2:178-187.

42. de Rooij M, Hamoen EH, Witjes JA, et al. Accuracy of Magnetic Resonance Imaging for Local Staging of Prostate Cancer: A Diagnostic Meta-analysis. Eur Urol. 2016; 70:233-45.

43. Dinneen E, Allen C, Strange T, et al. Negative mpMRI Rules Out Extra-Prostatic Extension in Prostate Cancer before Robot-Assisted Radical Prostatectomy. Diagnostics (Basel). 2022; 12.1057

44. Park KJ, Kim MH, Kim JK. Extraprostatic Tumor Extension: Comparison of Preoperative Multiparametric MRI Criteria and Histopathologic Correlation after Radical Prostatectomy. Radiology. 2020; 296:87-95.

45. Xu G, Xiang L, Wu J, et al. The accuracy of prostate lesion localization in cognitive fusion. Clinical Hemorheology and Microcirculation. 2020; 74:223-229.

46. Rais-Bahrami S, Siddiqui MM, Turkbey B, et al. Utility of multiparametric magnetic resonance imaging suspicion levels for detecting prostate cancer. J Urol. 2013; 190:1721-1727.

47. Bratan F, Niaf E, Melodelima C, et al. Influence of imaging and histological factors on prostate cancer detection and localisation on multiparametric MRI: a prospective study. Eur Radiol. 2013; 23:2019-29.

48. Girouin N, Mège-Lechevallier F, Tonina Senes A, et al. Prostate dynamic contrast-enhanced MRI with simple visual diagnostic criteria: is it reasonable? Eur Radiol. 2007; 17:1498-509.

Correspondence

Ana Sofia Araújo (Corresponding Author)
ana.sofia.araujo@hb.min-saude.pt

Sara Anacleto
sara.anacleto@hb.min-saude.pt

Ricardo Rodrigues
ricardo.matos.rodrigues@hb.min-saude.pt

Catarina Tinoco
catarina.sousa.tinoco@hb.min-saude.pt

Andreia Cardoso
andreia.filipa.cardoso@hb.min-saude.pt

Mariana Capinha
mariana.dias.capinha@hb.min-saude.pt

Vera Marques
vera.p.marques@hb.min-saude.pt

Paulo Mota
paulo.mota@hb.min-saude.pt

Hospital de Braga, Dept. of Urology, Braga, Portugal

João Serra
serrajoao.ricardo@gmail.com

School of Medicine, University of Minho, Dept. of Urology, Braga, Portugal

Conflict of interest: The authors declare no potential conflict of interest.